Geomechanics and Engineering, *Vol. 31, No. 6 (2022) 573-582*
https://doi.org/10.12989/gae.2022.31.6.573

Influence of geometric factors on pull-out resistance of gravity-type anchorage for suspension bridge

Hyunsung Lim[1], Seunghwan Seo[2], Junyoung Ko[3] and Moonkyung Chung*[2]

[1]*Department of Wind Power Business, Hanwha Corporation/E&C, Seoul 04541, Republic of Korea*
[2]*Department of Geotechnical Engineering Research, Korea Institute of Civil Engineering and Building Technology, Goyang-si, Gyeonggi-do 10223, Republic of Korea*
[3]*Department of Civil Engineering, Chungnam National University, Daejeon 34134, Republic of Korea*

(*Received July 13, 2022, Revised December 10, 2022, Accepted December 12, 2022*)

Abstract. The geometry of the gravity-type anchorage changes depends on various factors such as the installation location, ground type, and relationship with the upper structure. In particular, the anchorage geometry embedded in the ground is an important design factor because it affects the pull-out resistance of the anchorage. This study examined the effect of four parameters, related to anchorage geometry and embedded ground conditions, on the pull-out resistance in the gravity-type anchorage through two-dimensional finite element analysis, and presented a guide for major design variables. The four parameters include the 1) flight length of the stepped anchorage (*m*), 2) flight height of the stepped anchorage (*n*), 3) the anchorage heel height (*b*), and 4) the thickness of the soil (*e*). It was found that as the values of *m* increased and the values of *n* decreased, the pull-out resistance of the gravity-type anchorage increased. This trend is related to the size of the contact surface between the anchorage and the rock, and it was confirmed that the value of *n*, which has the largest change rate of the contact surface between the anchorage and the rock, has the greatest effect on the pull-out resistance of the anchorage. Additionally, the most effective design was achieved when the ratio of the step to the bottom of the anchorage (*m*) was greater than 0.7, and *m* was found to be an important factor in the pull-out resistance behavior of the anchorage.

Keywords: finite element analysis; geometric condition; gravity-type anchorage; pull-out resistance; suspension bridge

1. Introduction

In a suspension bridge, the load applied on the bridge is supported by the tensile force of cables, with the deck hanging below suspension cables with both ends fixed. It is a widely used long-span bridge structure because of its considerable advantages in terms of material properties and the height-spans ratio of the stiffening girder (Adanur *et al*. 2012, Lekidis *et al*. 2005, Gwon and Choi 2018, Lei *et al*. 2012, Han *et al*. 2019).

Suspension bridges are classified into earth-anchored and self-anchored bridges depending on the method of fixing the main cable (Deng *et al*. 2018, ASCE 1979) In earth-anchored suspension bridges, the main cable is fixed by positioning anchorages at both ends of the bridge, and in self-anchored suspension bridges, the main cable is fixed to the pier at the end of the bridge without installing a separate anchorage. The anchorage of earth-anchored suspension bridges is crucial for maintaining the stability of the entire bridge because a large load is applied while fixing the main cables (Li and Li 2006) Anchorages can be classified into gravity-type, tunnel-type, and rock-anchored type (Han *et al*. 2019, Lim *et al*. 2020, Lim *et al*. 2021, Seo *et al*. 2021).

Gravity-type anchorages are the most commonly applied type in Korea, with examples of such structures including the Namhae Bridge (1973), Gwangyang Bridge (2002), Yi sun-sin Bridge (2013), and Palyeong Bridge (2016). A gravity-type anchorage has a relatively reliable and strong resistance mechanism compared to other types because it considers the dead weight of the concrete body as the element of bearing capacity. In addition, active research has been conducted on resistance mechanisms such as frictional resistance between concrete and rock mass and passive resistance in front of the anchorage, and the design method of the gravity-type anchorage is relatively well-known. However, gravity-type anchorages have some drawbacks, in that a large quantity of concrete is needed and block placement and control of the heat of hydration are required for quality control of mass concrete. In addition, if a rock mass suitable for anchorage installation is found in a deep place, disadvantages arise, such as increase in the excavation volume, need for additional temporary retaining wall, and environmental damage in a large area.

To address these drawbacks, a stepped gravity-type anchorage can be used, in which the bottom of the anchorage is designed in the form of steps with a slope, securing the size of the body on the rear side for anchoring the cable strands while reducing the volume of excavation on the front side, thereby reducing the concrete quantity. However, in the stepped gravity-type anchorage design, the passive resistance of the front soil is not considered, necessitating the implementation of a conservative design. Moreover, there have been limited analyses on the resistance behavior of the inclination effect of the step

*Corresponding author, Ph.D.
E-mail: mkchung@kict.re.kr

ISSN: 2005-307X (Print), 2092-6219 (Online)

characteristics such as the slope, tread depth, and riser height.

Therefore, to consider the pull-out resistance in the design of a gravity-type anchorage, the inclination effect of steps was investigated according to the 1) flight length of the stepped anchorage (m), 2) flight height of the stepped anchorage (n), 3) the anchorage heel height (b), and 4) the thickness of the soil (e). A model for numerical analysis was developed considering the typical conditions of gravity-type anchorages, and based on the developed model, the pull-out resistance behavior of the anchorage was analyzed with respect to different conditions.

2. Problem definition

Gravity-type anchorages should be designed to effectively transfer the external force from the cable tension, the moment generated by the force, and the dead load of the anchor body and foundation required for resistance to the soil. For structural design of the gravity-type anchorage, the stability assessment must satisfy the following four criteria: ground bearing capacity, sliding, overturning, and displacement (Ministry of Land, Infrastructure and Transport 2016). For sliding, the external force in the lateral direction applied on the foundation should be less than the value of sliding resistance of the underside of the foundation multiplied by the resistance coefficient. The sliding resistance of the foundation can be calculated as follows

$$H_u = cA' + V\tan\phi \quad (1)$$

where, H_u is the sliding resistance of anchorage foundation (kN), c is the cohesion of the foundation soil (kN/m^2), A' is the area of the ground in contact by applied load condition (m^2), V is the axial force applied to the underside of foundation (kN), and ϕ is the internal friction angle of the foundation soil (°).

As for the anchorage design, environmental factors such as topographic conditions, bridge types, and landscape conditions need to be considered, and the embedded depth of the anchorage varies according to the depth and other conditions of the bearing layer, making it difficult to set a unified shape of the anchorage body in practice. That is, since the design of gravity-type anchorages requires complex consideration of various design issues, the shape of the resulting anchorage body differs for each design.

In addition, to improve workability in excavation and structural stability, the slope types of the bottom surface of the anchorage are classified into three types: stepped slope, single slope, and flat bottom (Fig. 1). In the case of the stepped slope, the sliding resistance of the underside of the foundation of the anchorage may be increased and the excavation work can be performed relatively easily (Fig. 1(a)). As for the single slope, sliding resistance can be reduced compared to the bench slope and slope excavation may be difficult. Furthermore, since rebar arrangement and concrete placement are performed on an inclined surface, workability is reduced (Fig. 1(b)). Lastly, in the case of the flat bottom surface, the workability is good, and the subgrade reaction applied on the front of the anchorage is increased by the cable load, but there is a disadvantage of excessive excavation volume (Fig. 1(c)).

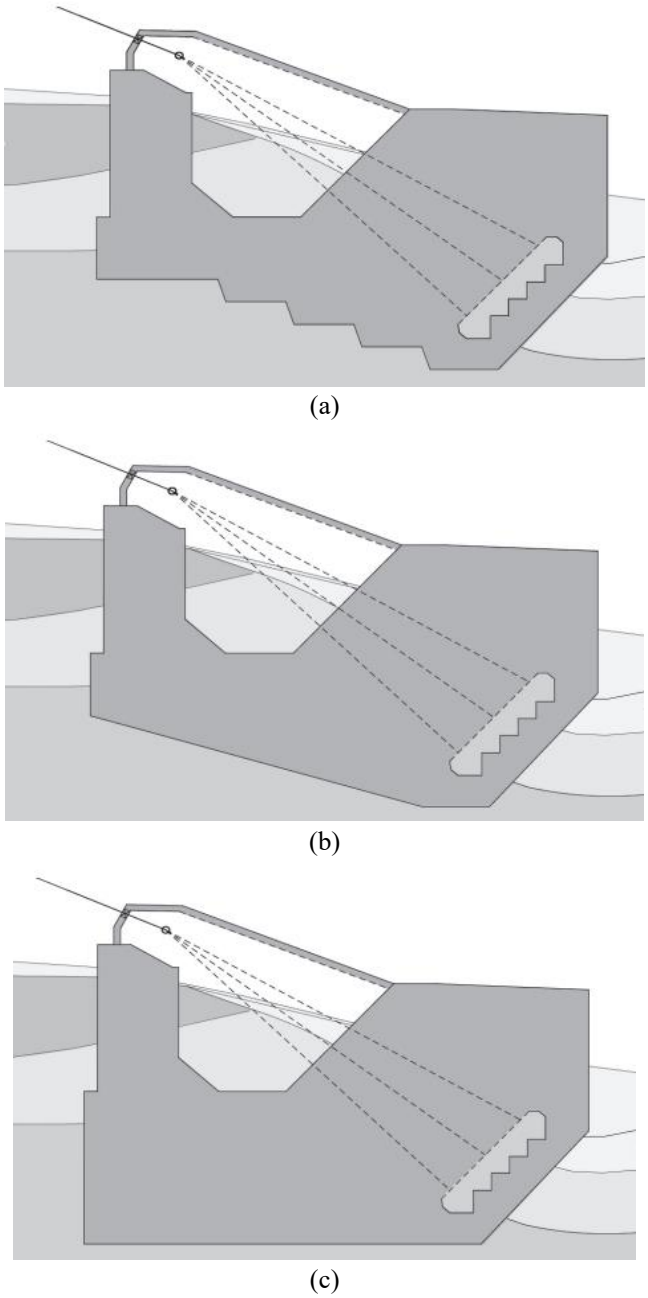

(a) (b) (c)

Fig. 1 Major types of bottom surface of the anchorage: (a) stepped slope bottom, (b) single slope bottom and (c) flat bottom

As mentioned above, due to 1) the complexity of the design considerations and 2) various types of slopes, most design cases have different types of anchorage cross-sections, leading to limited quantitative analysis on the sliding resistance of the anchorage. Therefore, in this study, several design cases were investigated and reasonable specifications for anchorage foundation were analyzed. Based on this analysis, the anchorage cross-section was generalized to consider 1) the complexity of the design considerations and 2) various types of slopes. Finally, a

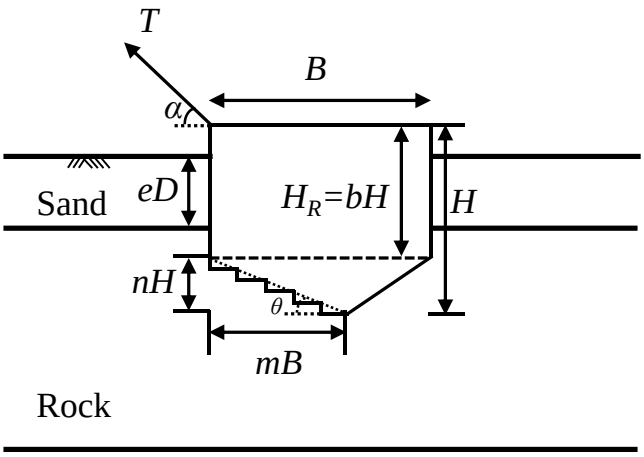

Fig. 2 Schematic model of a gravity-type anchorage

parametric study was performed considering various conditions using the generalized anchorage cross-section.

Because of the requirement for comprehensive design considerations, the anchorage cross-section has a complex shape and each design has a different geometry of the cross-section. Therefore, to analyze the pull-out resistance behavior of the anchorage according to the number of steps, the slope (width, height) of the steps, and the heel size, the gravity-type anchorage conditions were generalized as shown in Fig. 2. The basic dimensions of the anchorage were defined with width B and height H, and it was assumed that the cable tension T is applied at an angle of α. In addition, because there are too many embedded variables and excessive complexity to consider the shape of the top part of the anchorage in detail, a flat shape was assumed. In general, because the dead load of the anchorage is the most dominant factor influencing the behavior for gravity-type anchorages, the dead load, rather than the geometry of the upper part of the anchorage, was considered.

Soil conditions were simplified into two layers for modeling, of which the top layer was assumed as a soil layer and the bottom as soft rock layer, which is the bearing layer. The depth of anchorage embedment in the strata is defined as D, which is normalized by H, the total height of the anchorage. Additionally, the effect from the depth of the soil layer was normalized by D and expressed as the coefficient e.

To reflect the inclination effect of the steps, the effect of the step width was normalized by the anchorage width (B) and expressed as the coefficient m, and the effect of the step height was normalized by the anchorage height (H) and expressed in terms of the coefficient n. Therefore, the inclination angle θ of the steps is determined according to the change in m and n. In addition, to consider the effect on the asymmetry of the anchorage cross section, the height of the anchorage heel (the right side, not the steps) was defined as H_R, which was normalized by H and expressed as a coefficient b.

By using data from different suspension bridge cases in Korea, the range of reasonable values of the normalized coefficients was analyzed and the influencing factors and their ranges for the parametric study were determined as

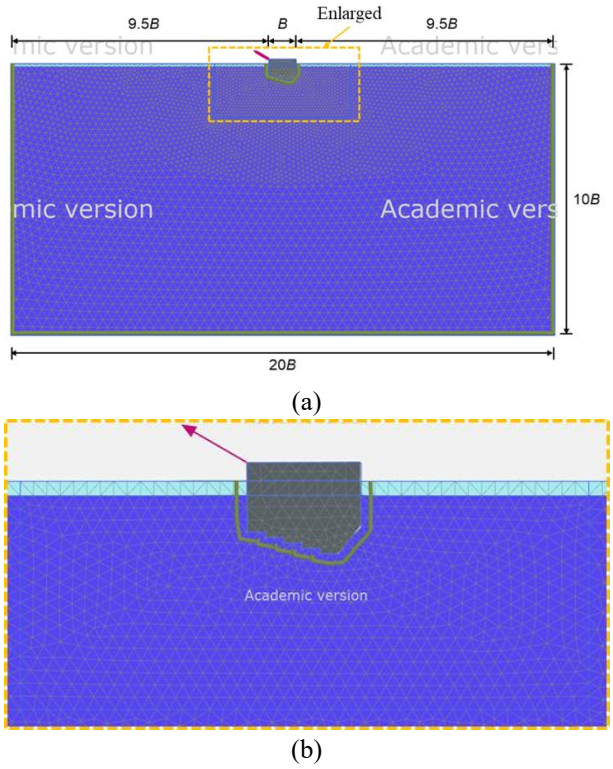

Fig. 3 Representative section of the FE model: (a) FE mesh of the entire section and (b) FE mesh of the enlarged part

presented in Table 1. Here, apart from the thickness of the soil layer (e), the geometry of the anchorage changes according to all variables. The flight of the stepped anchorage consists of 5 steps, and as the flight length and height change, the tread and rise of each step change proportionally.

3. Finite element analysis

In this study, we aim to analyze the pull-out resistance behavior under various geometric conditions using a generalized model for a gravity-type anchorage. For this parametric study, a finite element analysis (FEA) technique was applied, and the Plaxis 2D (2020) general-purpose geotechnical analysis software, was used for modeling under the plane strain condition.

3.1 Numerical modeling

Fig. 3 shows the analysis domain and FE mesh of the numerical model. As for the boundary conditions of the simulation, the range of the FE analysis was extended to the region with minimal effect on changes in the stress and displacement during the pull-out resistance behavior caused by the cable tension of the anchorage. For the left and right boundary boundaries, 10 times (10B) of the anchorage foundation width was applied to the left and right with the anchorage foundation as the center, and 10 times (10B) of the anchorage foundation width was applied to the bottom boundary.

Table 1 Parametric studies conducted in this study

Influencing factor	Range of factor values	Fixed conditions
flight length of the stepped anchorage (m)	0.5–1.0	n=0.3, e=0.2, 5 steps
flight height of the stepped anchorage (n)	0.0–0.5	m=0.8, e=0.2, 5 steps
the anchorage heel height (b)	0.5–1.0	m=0.8, n=0.3, e=0.2, 5 steps
the thickness of the soil layer (e)	0.0–0.5	m=0.8, e=0.3, 5 steps

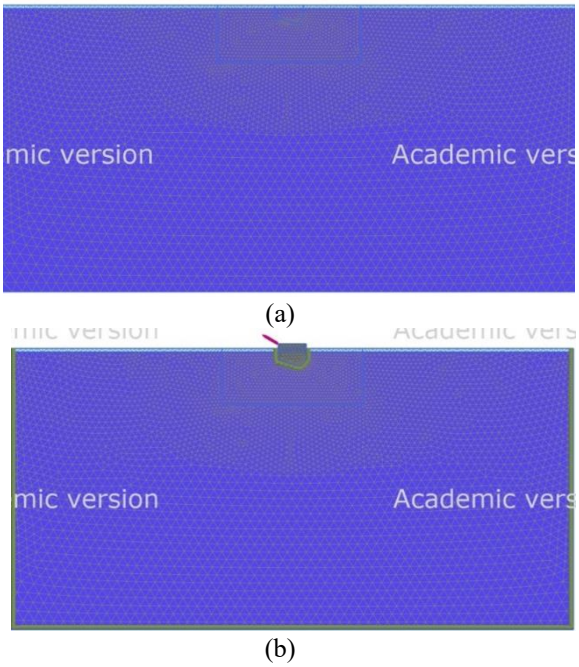

Fig. 4 Simulation process: (a) Step 1: soil stress simulation and (b) Step 2: installation of the anchorage and application of the external force

Table 2 Summary of material properties

Properties	γ (kN/m^3)	ν	E (MPa)	c (kPa)	ϕ (°)	R_{int}*
Dense Sand	18.5	0.35	40	0	30	0.67
Soft rock	23	0.25	1,300	100	37.5	1.0
Anchorage	17.8	0.2	28,000	-	-	-

*Rint is the value related to the interface between different materials

3.2 Material properties

The simulation model in this study is largely divided into the overlying soil layer, bearing layer, and anchorage. In this study, simulation was performed based on the assumptions that the overlying soil and bearing layers were composed of dense sand and soft rock, respectively. In addition, the Mohr–Coulomb plasticity model of soils has been used for the overlying soil and bearing layers, and the anchorage was simulated based on the linear elastic model. The Mohr-Coulomb model is one of the most widely used models in geotechnical engineering (Kim *et al.* 2020, Jaiswal and Rakesh 2022, Das *et al.* 2022, Karira *et al.* 2022). The material properties used for input data of the simulation model were determined by referring to the values reported in the geotechnical investigation reports of the Noryang Bridge, Palyeong Bridge, and Ulsan Bridge and the existing literature (Yooshin Co., Ltd. 2004a, b, 2009a, b, Choi *et al*. 2015, Ko *et al*. 2018, Ko *et al*. 2020, Reul *et al*. 2004). Table 2 outlines the properties of the materials used in the FEA of this study.

3.3 Description of simulation process

The angle of incidence (α) of the cable tension applied to the anchorage was fixed at 30°, and the displacement control method was applied for simulation to analyze the reaction force generated after inducing displacement at the interface of the anchorage model. The simulation process consisted of the following two steps (Fig. 4). In the first step, the initial stress of the soil was simulated. It is assumed to increase as $\sigma v=\gamma z$ according to the depth, and the horizontal stress (σ_h) was applied as a value obtained by multiplying the vertical stress by the lateral earth pressure coefficient (K_0). In the second step, the processes of anchorage installation and load application were performed, and the cable load was applied while controlling the anchorage displacement. At this time, displacement was generated until the reaction force no longer increased, and this state was assumed to be the ultimate state.

4. Results and discussion

4.1 Method of simulation result analysis

To analyze the pull-out resistance behavior with respect to the inclination effect of the steps of the bottom surface of foundation of the gravity-type anchorage, simulation cases were selected as presented in Table 1 and a parametric study was performed. A quantitative evaluation of the pull-out resistance behavior was conducted by plotting the displacement-reaction force curves for all geometric conditions of each simulation case. To quantify the effect on the anchorage behavior in each case, the magnitudes of the reaction force at displacements of 0.002B (0.2% of anchorage width), 0.004B (0.4% of anchorage width), and 0.006B (0.6% of anchorage width) were used as the reference values, as shown in Fig. 5. The magnitudes of the reaction force for the respective values of displacement were compared to determine the minimum value RF_{min}, and the ratio with the corresponding reaction force was calculated. Accordingly, a quantitative evaluation of the pull-out resistance behavior was performed by analyzing

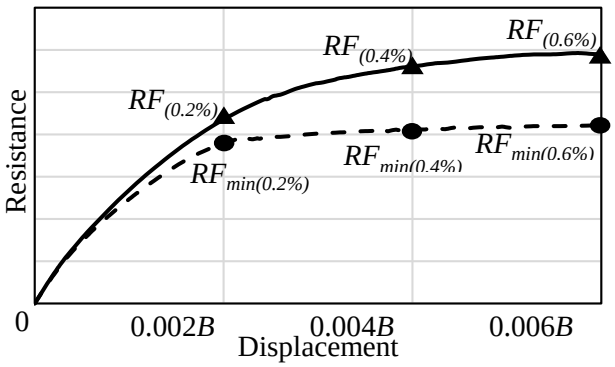

Fig. 5 Result analysis

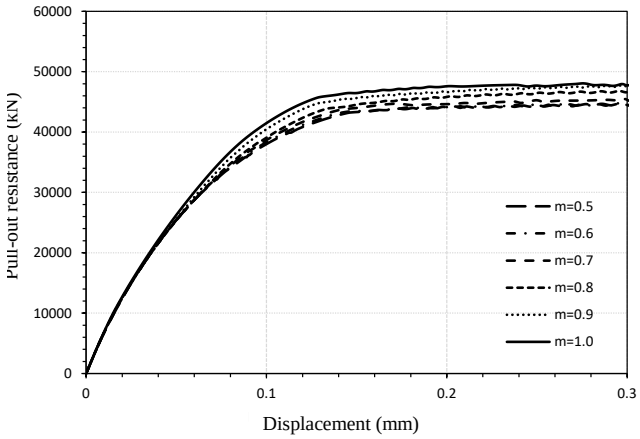

Fig. 6 Displacement-pull-out resistance curve according to *m*

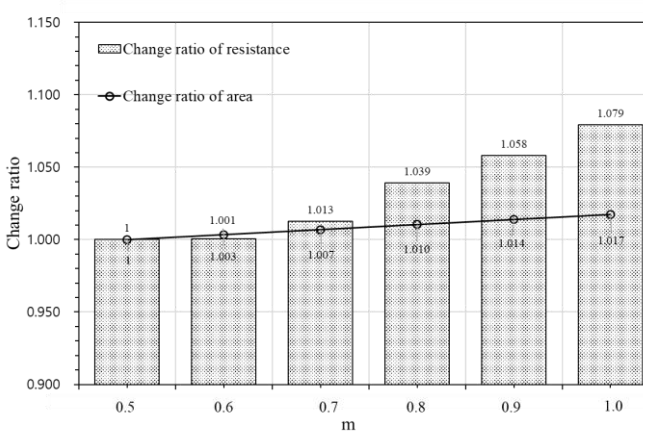

Fig. 7 Displacement-pull-out resistance curve according to *m*

the degree of change (increase/decrease) compared to the minimum value.

However, it is difficult to evaluate the pull-out resistance of the anchorage by only using the displacement-reaction force curves. This is because the dead load of the anchorage structure of the gravity-type anchorage significantly affects the anchorage behavior. Therefore, the analysis in terms of the dead load of the anchorage structure is also required. Different values of the dead load were compared by calculating the rate of change for the cross-sectional area.

Table 3 Anchorage cross-sectional shape according to *m* (*n*=0.3, *e*=0.2, 5 steps)

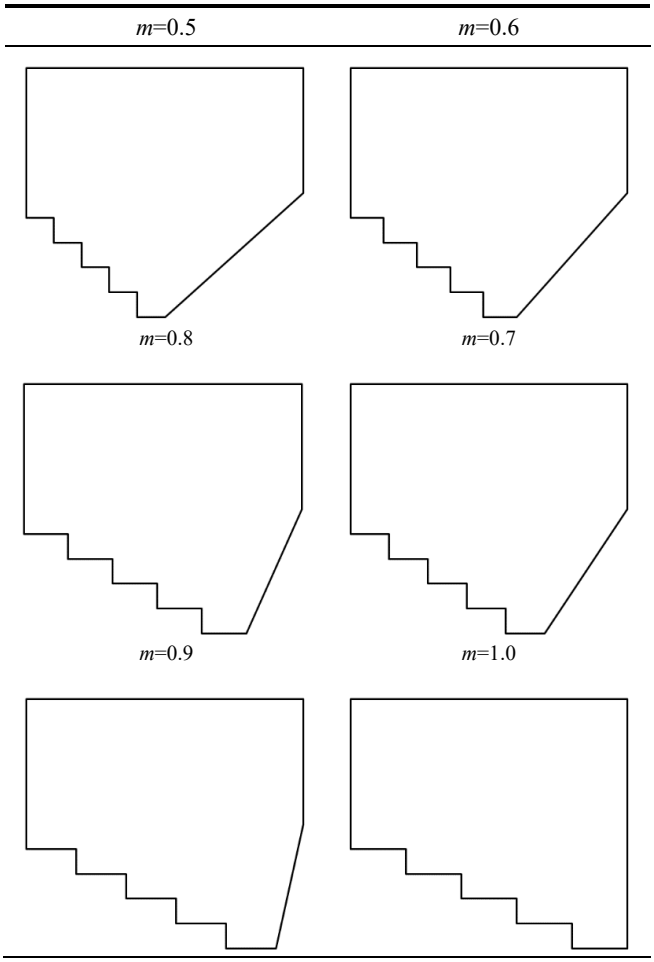

4.2 Flight length of the stepped anchorage (m)

To analyze the effect of flight length of the stepped anchorage, a total of six cases (stepped section) were analyzed by simulation. Table 3 shows the anchorage cross-sectional shape according to *m*. The flight length of the stepped anchorage (factor *m*) was varied from 0.5 to 1.0; *m* = 0.5 represents the case when the end of the steps is located at the center of the anchorage, and *m* = 1 represents the case when the end of the steps is located at the right end of the anchorage. In the simulation, the coefficient of the effect of the step height was kept constant at *n* = 0.3 and that of the effect of overlying soil layer was *e* = 0.2.

Fig. 6 demonstrates the displacement-pull-out resistance curve with respect to *m*. The cases of *m* = 0.5 and *m* = 0.6 show very similar patterns, and the value of the ultimate pull-out resistance increases from *m* = 0.7. When *m* = 1.0, the ultimate pull-out resistance value is the largest. According to these results, the greater the flight length, the greater the pull-out resistance of the anchorage.

To analyze the ratio of resistance and change of the cross section of the anchorage, the result values are summarized in Fig. 7. Since ultimate pull-out resistance was expressed at a displacement of 0.002*B*, the change ratio of displacement of 0.002*B* was compared. Based on the

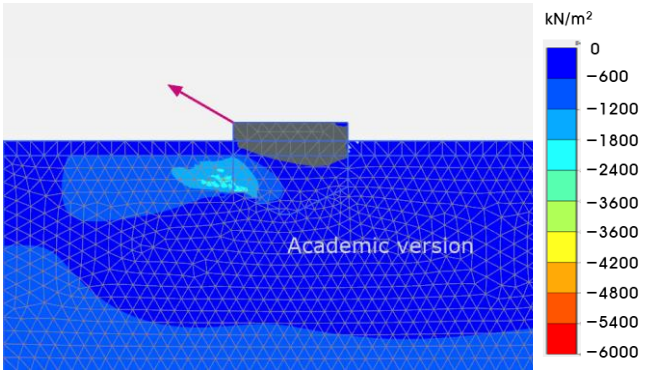

(a)

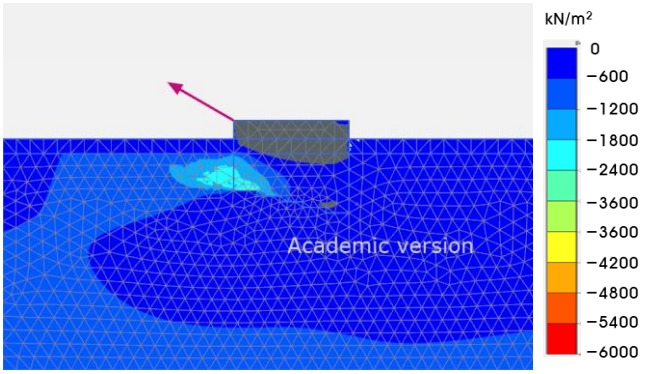

(b)

Fig. 8 Horizontal stress contours: (a) m= 0.5 and (b) m= 1.0

results, the cross section increased by 0.3% for m = 0.6, compared to that for m = 0.5. However, the change in the pull-out resistance is smaller than this ratio, indicating that the step effect is insignificant. For m = 0.7 or more, the increase in pull-out resistance is greater than the increase in cross section. Therefore, m = 0.7–1.0 is considered to be effective for design. When m = 1.0, the pull-out resistance was larger by 6.2% compared to the case when m = 0.5, indicating that the step effect was the largest at m = 1.0. Fig. 8 shows the respective horizontal stress contours when m is 1.0 and 0.5. It can be seen that when m is 1.0, the stress is greater than when it is 0.5.

4.3 Flight height of the stepped anchorage (n)

Simulations for a total of six cases (stepped section) were performed to analyze the effect of the flight height of the stepped anchorage (n). Table 4 shows the anchorage cross-sectional shape according to n. Factor n was varied from 0.0 to 0.5; n = 0.0 indicates no step and a rectangular anchorage, and n = 0.5 represents the case when the flight height reaches the middle point of the entire height of the anchorage. In the simulation, the coefficient of the effect of the step width was kept constant at m = 0.8 and the coefficient of the effect of overlying soil layer was e = 0.2.

Fig. 9 presents the displacement-pull-out resistance curve with respect to the flight height. The case of n = 0.5 was excluded because the simulation did not show convergence to the ultimate state. The effect of the flight height is larger than the effect of the flight length. This is because the cross section of the gravity-type anchorage

Table 4 Anchorage cross-sectional shape according to n (m=0.8, e=0.2, 5 steps)

n = 0.0	n = 0.1
	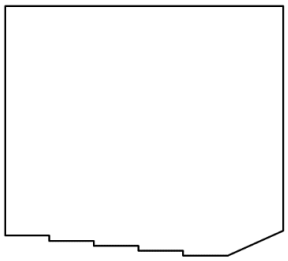
n = 0.2	n = 0.3
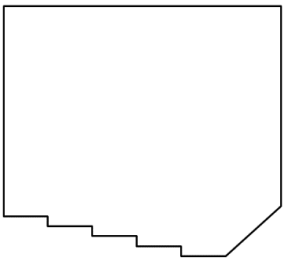	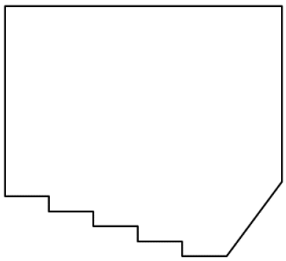
n = 0.4	n = 0.5
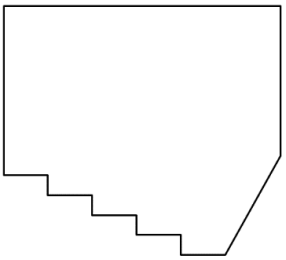	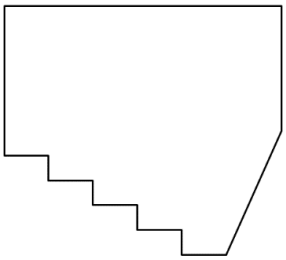

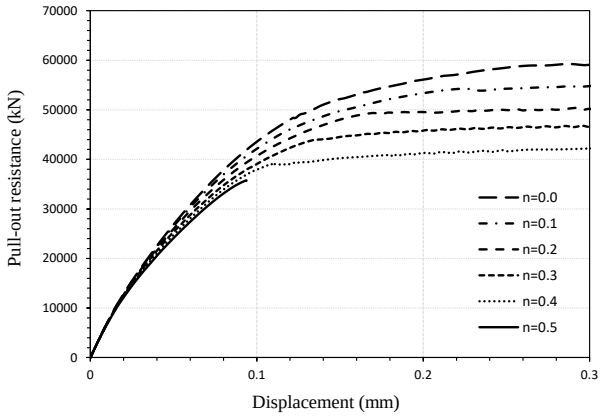

Fig. 9 Displacement-pull-out resistance curve according to n

varies greatly according to the flight height, thus substantially affecting the pull-out resistance behavior. When n = 0.4, the anchorage has the smallest cross section, and when n = 0.0, it has the largest cross section with a rectangular shape without steps. When examining the ultimate pull-out resistance value for each case, a difference was observed between each case in an almost constant ratio.

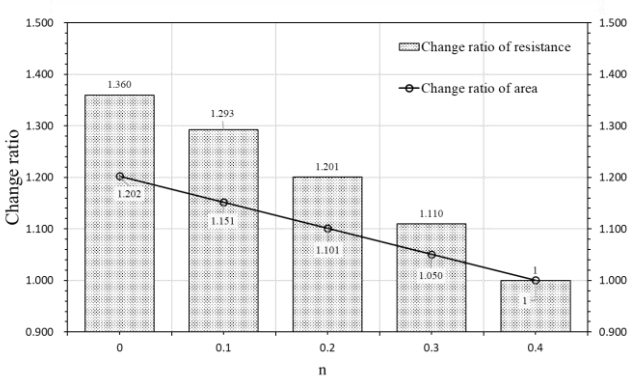

Fig. 10 Change ratio of resistance and area according to *n*

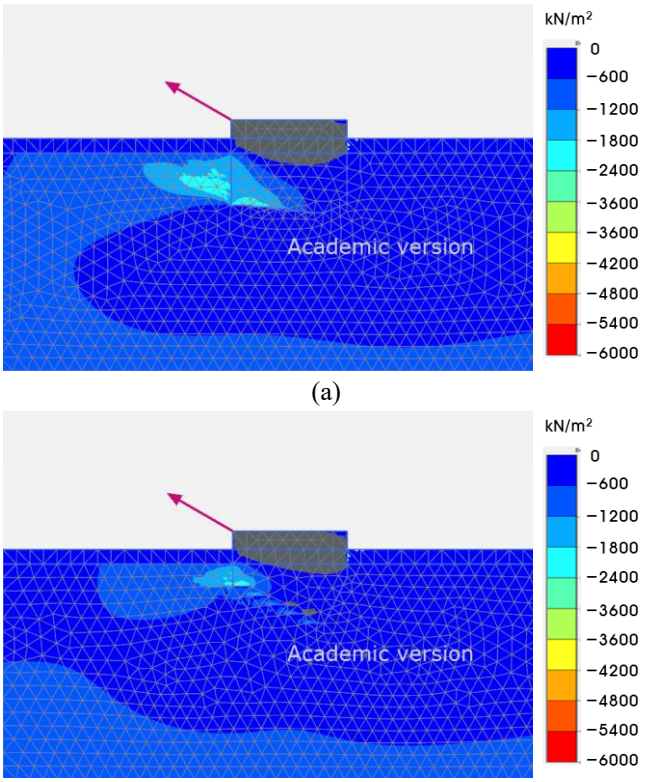

(a)

(b)

Fig. 11 Horizontal stress contours: (a) *n*= 0.1 and (b) *n*=0.5

If the flight length is kept constant, the pull-out resistance increases with an increase in the flight height.

The ratio of resistance and change of the cross section of the anchorage can be analyzed using the result values summarized in Fig. 10. As mentioned earlier, the cross section of the anchorage with respect to the flight height increased by 5–20 % compared to the minimum case, indicating that the increase was larger than other geometric factors. Fig. 11 shows the respective horizontal stress contours when *n* is 0.1 and 0.5. It can be seen that when *n* is 0.1, the stress is greater than when it is 0.5.

4.4 The anchorage heel height (b)

To analyze the effect of asymmetry in the anchorage geometry, a total of six cases (stepped section) were simulated, wherein the starting points of the anchorage steps and the heel are not the same. Table 5 shows the anchorage cross-sectional shape according to *b*. In this simulation, the coefficient *b* was changed from 0.5 to 1.0 to vary the height of the right side of the anchorage heel. When *b* = 0.5, the starting point of the heel is located in the middle of the total height of the anchorage, and when *b* = 1.0, the starting point is the same as the height of the bottom of the steps. In the simulation, the coefficient of step width effect was kept constant at *m* = 0.8, the coefficient of step height effect was *n* = 0.3, and the coefficient of overlying soil layer effect was *e* = 0.2.

Table 5 Anchorage cross-sectional shape according to *b* (*m*=0.8, *e*=0.2, 5 steps)

b=0.5	*b*=0.6
b=0.7	*b*=0.8
b=0.9	*b*=1.0

Fig. 12 shows the displacement-pull-out resistance curve with respect to the height of the anchorage heel. The cases of *b* = 0.5 and *b* = 0.6 were excluded because the simulation did not converge to the ultimate state, making it difficult to compare these cases with other cases. When *b* = 0.7, the difference in the ultimate pull-out resistance value was not large, and the pull-out resistance increased with *b*.

To analyze the ratio of resistance and change of the cross section of the anchorage, the values were obtained, as summarized in Fig. 13. From the results, the cross section increases with *b*. It can be seen that the difference between the change ratio of the pull-out resistance and the change

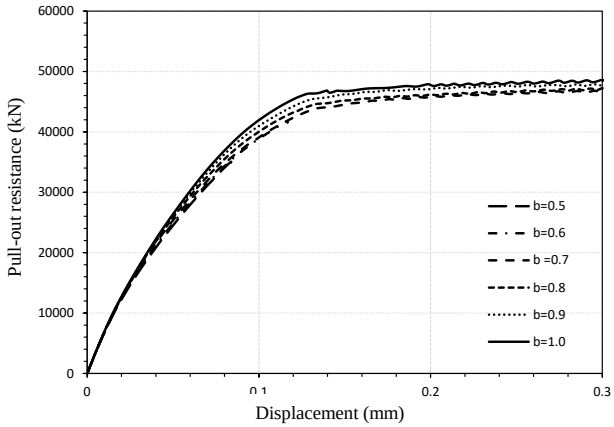

Fig. 12 Displacement-pull-out resistance curve according to *b*

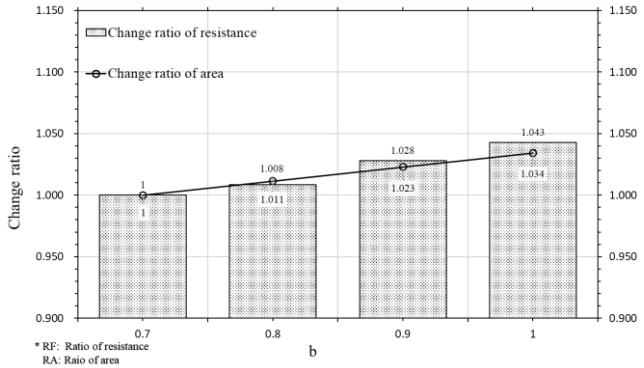

Fig. 13 Change ratio of resistance and area according to *b*

ratio of the cross section according to the change of *b* is not large. Therefore, it was found that the increase in the pull-out resistance according to the change of the height of the anchorage heel affects the size of the cross section, and the influence of the height of the anchorage heel is insignificant. Fig. 14 shows the respective horizontal stress contours when *b* is 0.7 and 1.0. It can be seen that when *b* is 0.7, the stress is greater than when it is 1.0.

4.5 The thickness of the soil layer (e)

The gravity-type anchorage of a suspension bridge is characterized by the selection of the location and design, considering the site conditions. Therefore, the stratum conditions should be analyzed because these conditions may vary in actual sites. Assuming a dense sandy soil layer in the overlying soil layer and a soft rock layer in the bearing layer, a total of six cases (stepped section) were considered to analyze the effect on the height of the sandy soil layer (or embedded depth of anchorage). The coefficient *e*, which represents the effect of the overlying soil layer, was varied from 0.0 to 0.5. Where $e = 0.0$ represents the case where the soil layer does not exist and all of the anchorage is embedded in the rock layer, and $e = 0.5$, represents the case where half of the embedded depth of anchorage is in soil layer and the other half is in the rock

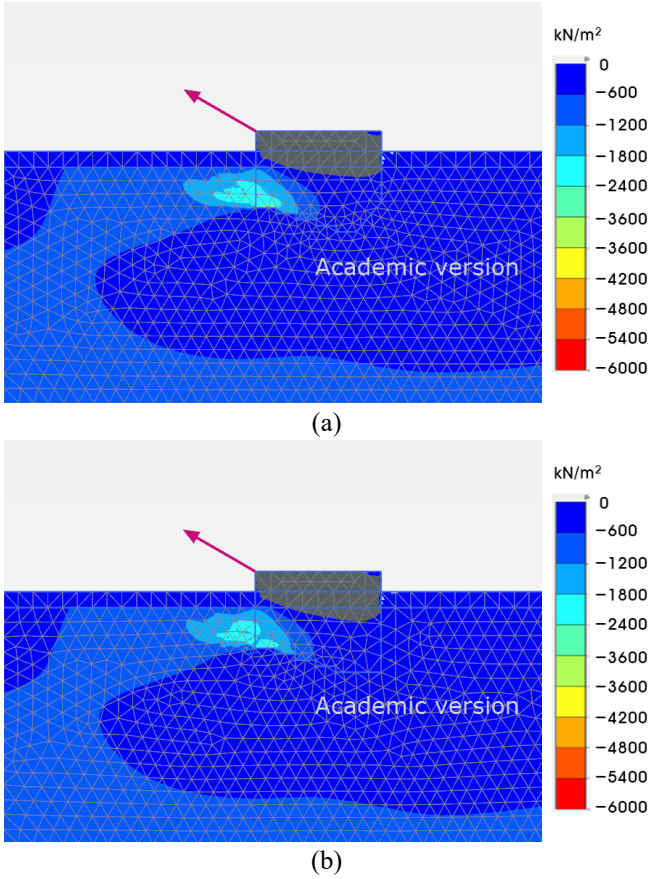

Fig. 14 Horizontal stress contours: (a) *b*= 0.7 and (b) *b*= 1.0

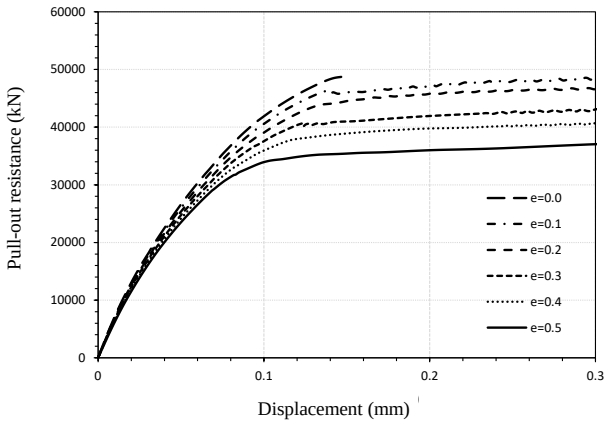

Fig. 15 Displacement-pull-out resistance curve according to *e*

layer. In the simulation, the coefficient of the effect of the step width was maintained constant at $m = 0.8$ and the coefficient of the effect of the step height at $n = 0.3$. That is, the anchorage geometry is fixed and only the strata condition varies in the simulation.

Fig. 15 presents the displacement-pull-out resistance force curve with respect to the depth of the overlying soil layer. For $e = 0.0$, the analysis did not converge to the ultimate state; thus, this case was excluded. As the depth of the overlying soil layer decreases, the ultimate pull-out resistance tends to increase. This is because the resistance to

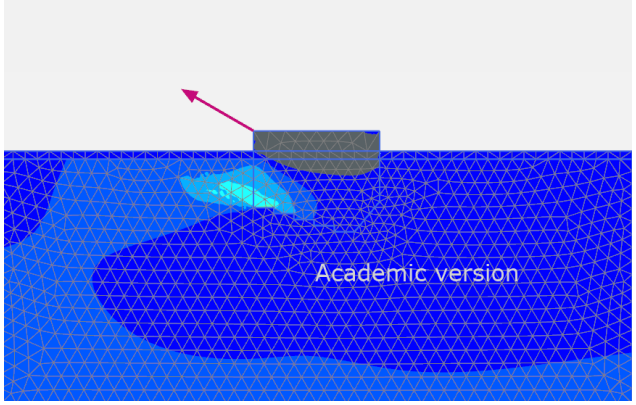

(a)

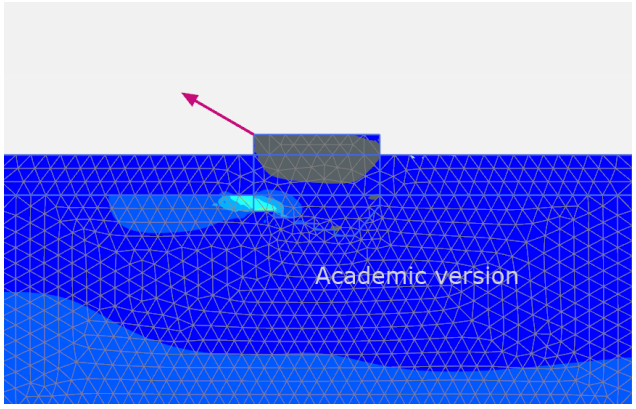

(b)

Fig. 16 Horizontal stress contours: (a) e= 0.1; (b) e=0.5

anchorage pull-out is increased, and the passive resistance in the pull-out direction is larger in the rock layer than in the soil layer. When examining the ultimate pull-out resistance for each case, a difference can be observed in an almost constant ratio between each case. In the simulation, since the geometry of the anchorage does not change, the cross section of the anchorage does not change. The results demonstrate that as e becomes smaller (increase in the embedment depth in the rock), the pull-out resistance increases. Further, the results indicate that the embedment depth in the rock is the most influencing factor in the pull-out resistance behavior of the anchorage. Fig. 16 shows the respective horizontal stress contours when e is 0.1 and 0.5.

5. Conclusions

This study investigated the changes of the pull-out resistance of the embedded part in the gravity-type anchorage based on its geometric parameters using the FEA. To quantitatively evaluate the shape and ground conditions of complex gravity-type anchorages, the cross-section of the anchorage was generalized. The pull-out resistance of the gravity-type anchorage was analyzed according to the 1) flight length of the stepped anchorage (m), 2) flight height of the stepped anchorage (n), 3) anchorage heel height (b), and 4) thickness of the soil (e). The slope types of the bottom surface of the anchorage were classified into three types: stepped slope, single slope, and flat bottom. Once the required pull-out resistance was achieved, the flat bottom types were not applied to the design for economic reasons. It was found that the pull-out resistances of the stepped slope and single slope types are similar. However, the stepped slope type has a high level of difficulty in excavation, and therefore the single slope type was found to be best option. Based on the findings of this study, the following conclusions can be drawn:

1. The pull-out resistance of the gravity-type anchorage increases as flight length of the stepped anchorage (m) increases because of the change in area between the bedrock and the bottom of the anchorage. Additionally, when m = 0.7 or greater, the pull-out resistance is greater than that in the dead load of the anchorage; thus, the anchorage geometry with m = 0.7 to 1.0 is considered to be effective.
2. It was found that the shorter flight height of the stepped anchorage (n), the greater the resistance of the anchorage. For the depth of the overlying soil layer (embedment depth in the rock, e), as e decreases (increase in the embedment depth in the rock), the pull-out resistance increases. This trend appears to be due to the increase of the contact area between the bedrock and the front part of the anchorage. It was also found that the effect of the anchorage heel height (b) on the pull-out resistance was negligible.
3. Among the influencing factors carried out in this study, the change in the pull-out resistance of the anchorage due to the change of n and e was large. Therefore, it is shown that the resistance area of the front part of the anchorage has the most dominant influence on the pull-out resistance.

Acknowledgments

This research was supported by a grant from the project “Development of Smart Complex

Solution for Large Deep Underground Space Using Artificial Intelligence” which was funded by the Korean Institute of Civil Engineering and Building Technology (KICT) and the Construction Technology Research Program (22SCIP-C151438-04) funded by the Ministry of Land, Infrastructure, and Transport of the Korean government.

References

Adanur, S., Gunaydin, M., Altunisik, A.C. and Sevim, B. (2012), “Construction stage analysis of Humber suspension bridge”, *Appl. Math. Model.*, **36**(11), 5492-5505. https://doi.org/10.1016/j.apm.2012.01.011.

ASCE (1979), “Long span of suspension bridge: history and performance”, *Proceedings of the ASCE National Conventions*, Boston, MA, USA.

Cho, J., Lim, H., Jeong, S. and Kim, K. (2015), “Analysis of lateral earth pressure on a vertical circular shaft by considering the 3D arching effect”, *Tunn. Undergr. Sp. Tech.*, **48**, 11-19. https://doi.org/10.1016/j.tust.2015.01.002.

Das, S., Halder, K. and Chakraborty, D. (2022), “Seismic bearing

capacity of shallow embedded strip footing on rock slopes", *Geomech. Eng.*, **30**(2), 123-138. https://doi.org/10.12989/gae.2022.30.2.123.

Deng, Y., Li, A., Chen, S. and Feng, D. (2018), "Serviceability assessment for long-span suspension bridge based on deflection measurements", *Struct. Control Health Monit.*, **25**(11), 1-23. https://doi.org/10.1002/stc.2254.

Gwon, S.G. and Choi, D.H. (2018), "Static and dynamic analyses of a suspension bridge with three-dimensionally curved main cables using a continuum model", *Eng. Struct.*, **161**, 250-264, 2018. https:/doi.org/ 10.1016/j.engstruct.2018.01.062.

Han, Y., Liu, X., Wei, N., Li, D., Deng, Z., Wu, X. and Liu, D. (2019), "A comprehensive review of the mechanical behavior of suspension bridge tunnel-type anchorage", *Adv. Mater. Sci. Eng.*, **2019**, 1-9. https://doi.org/10.1155/2019/3829281.

Jaiswal, A. and Kumar, R. (2022), "Finite element analysis of granular column for various encasement conditions subjected to shear load", *Geomech. Eng.*, **29**(6), 645-655. https://doi.org/10.12989/gae.2022.29.6.645.

Karira, H., Kumar, A., Ali, T.H., Mangnejo, D.A. and Mangi, N. (2022), "A parametric study of settlement and load transfer mechanism of piled raft due to adjacent excavation using 3D finite element analysis", *Geomech. Eng.*, **30**(2), 169-185. https://doi.org/10.12989/gae.2022.30.2.169.

Kim, Y., Lim, H. and Jeong, S. (2020), "Seismic response of vertical shafts in multi-layered soil using dynamic and pseudo-static analyses", *Geomech. Eng.*, **21**(3), 269-277. https://doi.org/10.12989/gae.2020.21.3.269.10.12989.

Ko, J., Cho, J. and Jeong S. (2018), "Analysis of load sharing characteristics for a piled raft foundation", *Geomech. Eng.*, **16**(4), 449-461. https://doi.org/10.12989/gae.2018.16.4.449.

Ko, J., Kim, S., Kim, S. and Seo, H. (2020), "Utilizing building foundations as micro-scale compressed air energy storage vessel: Numerical study for mechanical feasibility", *J. Energy Storage*, **28**, 101225. https://doi.org/10.1016/j.est.2020.101225.

Lei, J.Q., Zheng, M.Z. and Xu G.Y. (2012), Suspension Bridge Design, China Communication Press, Beijing, China.

Lekidis, V., Tsakiri, M., Makra, K., Karakostas, C., Klimis, N. and Sous, I. (2005), "Evaluation of dynamic response and local soil effects of the Evripos cable-stayed bridge using multi-sensor monitoring systems", *Eng. Geol.*, **79**(1-2), 43-59. https://doi.org/10.1016/j.enggeo.2004.10.015.

Li, J.P. and Li, Y.S. (2006), "Research on displacement of anchorage of suspension bridge", *Ground Modification and Seismic Mitigation, Proceedings of the GeoShanghai Conference, Shanghai*, China, June.

Lim, H., Seo, S., Lee, S. and Chung, M. (2020), "Analysis of the passive earth pressure on a gravity-type anchorage for a suspension bridge", *Geo. Eng.*, **11**, 1-7. https://doi.org/10.1186/s40703-020-00120-5.

Lim, H., Seo, S., Ko, J. and Chung, M. (2021), "Effect of joint characteristics and geometries on tunnel-type anchorage for suspension bridge", *Appl. Sci.*, **11**(24), 11688. https://doi.org/ 10.3390/app112411688.

Ministry of Land, Infrastructure and Transport (MOLIT) (2016), "Korean highway bridge design standard (limit state design)", (in Korean), Seoul, South Korea.

PLAXIS (2020), PLAXIS 2D Reference Manual; Bentley: Exton, PA, USA.

Reul, O. and Randoplh, M.F. (2004), "Design strategies for piled rafts subjected to nonuniform vertical loading", *J. Geotech. Geoenviron. Eng.*, **130**(1), 1-13. https:/doi.org/ 10.1061/(ASCE)1090-0241(2004)130:1(1).

Seo, S., Lim, H. and Chung, M. (2021), "Evaluation of failure mode of tunnel-type anchorage for a suspension bridge via scaled model tests and image processing", *Geomech. Eng.*, **24**(5), 457-470. https://doi.org/10.12989/gae.2021.24.5.457.

Yooshin Co., Ltd. (2004a), Noryang Bridge Grand Bridge and Access Road Private Proposal Project: Basic Design Report (in Korean).

Yooshin Co., Ltd. (2004b), Noryang Bridge Grand Bridge and Access Road Private Proposal Project: Geotechnical Soil Report (in Korean).

Yooshin Co., Ltd. (2009a), Paryoung Grand Bridge and Access Road Private Proposal Project: Basic Design Report (in Korean).

Yooshin Co., Ltd. (2009b), Paryoung Grand Bridge and Access Road Private Proposal Project: Geotechnical Soil Report (in Korean).

Yooshin Co., Ltd. (2009a), Ulsan Grand Bridge and Access Road Private Proposal Project: Basic Design Report (in Korean).

Yooshin Co., Ltd. (2009b), Ulsan Grand Bridge and Access Road Private Proposal Project: Geotechnical Soil Report (in Korean).

IC